nature reviews physics
https://doi.org/10.1038/s42254-026-00950-9

Perspective

Check for updates

Radioactive molecules as laboratories of fundamental physics

A. Jadbabaie[1,2], S. Ebadi[1,2], R. F. Garcia Ruiz[1] ✉, N. R. Hutzler[3], A. M. Jayich[4] & J. T. Singh[5]

Abstract

Radioactive molecules provide a new platform in the search for new physics, at energy scales complementary to those probed by high-energy particle colliders. By combining enhancements from nuclear properties with the sensitivity and control offered by molecular structure, experiments with radioactive molecules offer great reach in the search for physics beyond the standard model. Progress in this field is being driven by advances in the production and control of radioactive molecules, alongside the development of new experimental tools and theoretical techniques. In this Perspective, we discuss the current status and future prospects of this rapidly developing, interdisciplinary field at the intersection of nuclear physics, atomic and molecular physics and particle physics.

Sections

[1]Department of Physics, Massachusetts Institute of Technology, Cambridge, MA, USA. [2]Department of Physics, Harvard University, Cambridge, MA, USA. [3]Division of Physics, Mathematics, and Astronomy, California Institute of Technology, Pasadena, CA, USA. [4]Department of Physics, University of California, Santa Barbara, CA, USA. [5]Facility for Rare Isotope Beams, Michigan State University, East Lansing, MI, USA. ✉e-mail: rgarciar@mit.edu

Introduction

A goal of modern physics is to discover new physics beyond the standard model. Despite its remarkable success at describing elementary particles and their interactions, the standard model cannot explain open questions about the origin and evolution of the Universe. Experimental searches for beyond-standard model physics are ongoing at three frontiers: the energy frontier, in which colliders such as the Large Hadron Collider (LHC) directly probe new particles and forces[1,2]; the intensity frontier, with studies of neutrinos and rare processes[3]; and the precision frontier, in which low-energy measurements provide a powerful and complementary approach[4,5]. Although the LHC is sensitive to new physics at the teraelectronvolt scale, precision measurements can indirectly probe much higher energy scales by measuring minute physical effects associated with the presence of undiscovered, symmetry-violating particles or forces[4].

One of the most pressing mysteries is the observed imbalance between matter and antimatter. According to the known laws of physics, the Big Bang should have produced equal amounts of both; however, observations reveal that the visible Universe consists almost entirely of matter, with antimatter contributing at most one part per billion[6]. Possible mechanisms behind this imbalance involve processes, governed by yet-to-be discovered particles in the early Universe that break fundamental, discrete symmetries of nature and hence produce more matter than antimatter[7,8]. The conjecture of such processes has motivated experimental and theoretical efforts to characterize the laws of physics under fundamental symmetries of charge conjugation (C), parity reversal (P) and time reversal (T). Extensions beyond the standard model generally introduce interactions that break fundamental symmetries, unless symmetry conservation is explicitly imposed[9,10].

Once a symmetry is broken at high energies, its effects can be traced through a 'tower' of effective field theories (EFTs)[11–14] to low energies, manifesting as symmetry-violating electromagnetic properties of nucleons, atoms and molecules[5,15,16]. The most prominent example of such a property is a permanent electric dipole moment (EDM) of a fundamental particle[17], which the Wigner–Eckart theorem dictates must be aligned with the intrinsic spin of the particle. The correlation of spin pseudovector and electric dipole vector violates P and T symmetries, which by the CPT theorem implies violation of charge–parity (CP) symmetry.

Within the standard model, only the weak force is known to violate C, P and CP symmetries individually[5]. However, EDMs induced by the weak force remain unobserved, as standard model contributions are at least six orders of magnitude below the current experimental sensitivity[5,18–20]. CP violation (CPV) can also, in principle, occur in the strong force, through the effective vacuum angle $\bar{\theta}$ in the standard model Lagrangian[21], $\mathcal{L}_{\bar{\theta}} \propto \bar{\theta}$. Because $\mathcal{L}_{\bar{\theta}}$ is non-perturbative, its effects vanish for high-energy colliders, and $\bar{\theta}$ must be probed by low-energy physics, such as EDMs. At present, experiments have found no evidence for CPV in the strong force, and bounds on the neutron EDM[22] have constrained the value of $\bar{\theta} < 10^{-10}$. Known as the strong CP problem, this striking observation of an unnaturally small unitless parameter, even after including radiative corrections[23], is a major puzzle of modern physics and an important motivation for quantum chromodynamics (QCD) axion models[24–27].

Within atoms and molecules, the presence of CPV, that is, an EDM, leads to small energy shifts that are amplified in heavy species owing to interactions between finite-size nuclei and relativistic, core-penetrating electrons. In particular, polar molecules — which break spherical symmetry and are highly polarizable — exhibit large internal fields and strong gradients that substantially amplify EDM signals compared with those in atoms[4,17]. Progress in bringing molecular complexity under control[28,29] has enabled >100× more precise bounds on the electron EDM in the past decade[30,31], substantially constraining various new physics models at or beyond the direct detection reach of particle colliders[17,32–36].

Molecular EDM searches have focused primarily on leptonic EDMs, owing to both their simpler hyperfine structure and straightforward theoretical interpretation compared with composite hadrons. However, with progress on the production and study of radioactive molecules in recent years[37–39], state-of-the-art measurements of hadronic CP-violating moments are now within reach, targeting orders of magnitude improvements in CPV sensitivity. Exploring the hadronic sector provides access to a broader range of new physics sources, beyond those constrained by lepton EDM measurements alone, including sensitivity to the strong CP problem[5,16].

Specifically, radioactive molecules containing pear-shaped (octupole-deformed) nuclei[40] offer a promising new platform for precision measurements of fundamental symmetry violation[38]. Certain heavy radioactive nuclei — such as ^{223}Fr, ^{225}Ra, ^{227}Th and ^{229}Pa — are either confirmed or suspected to exhibit octupole deformation and nearly degenerate ($\Delta E \lesssim 100$ keV) opposite-parity nuclear states, which can enhance CPV nuclear properties by more than three orders of magnitude when compared with stable nuclei[5,41]. By embedding an octupole-deformed nucleus in a polar molecule, the additional molecular enhancement further amplifies observable CPV, yielding energy shifts that can be more than six orders of magnitude larger than those in stable atoms[4,38]. Moreover, the rich internal structure of molecules can enable internal state-based co-magnetometry and quantum control protocols that reduce systematic uncertainties and increase effective sensitivity[29,42–44]. Together, these features make radioactive molecules uniquely attractive for researching fundamental symmetries beyond the reach of current colliders[4,5,15–17,38]. With many orders of magnitude separating current bounds and standard model predictions, any non-zero EDM measurement would be evidence of new physics, whereas continued null results further tighten bounds on hypothetical new particles and forces. In either outcome, the enhanced sensitivity and broad reach of precision measurements with radioactive molecules position them to have a leading role in exploring the fundamental laws of nature.

In this Perspective, we outline how EDMs can be measured indirectly via the nuclear Schiff moment, and how this moment is enhanced by octupole deformation of nuclei. We then discuss how to interpret measurements via EFTs and the energies that can be accessed. Next, we survey the experimental techniques for producing, trapping and measuring radioactive molecules and the challenges these techniques face. We conclude by outlining the relevance of radioactive molecules in other fields and future directions.

Symmetry-violating nuclear properties

In atoms and molecules, direct nuclear EDMs, induced by $\bar{\theta}$ or new physics, are partially screened by the orbiting electrons, a result known as Schiff's theorem[45]. Therefore, rather than measuring the nuclear EDM directly, hadronic CPV experiments probe the nuclear Schiff moment $\mathbf{S}$, a residual CPV vector moment arising from relativistic dynamics and finite nuclear-size effects that evade electronic screening[46–48]. CPV in atoms and molecules can also be observed via an electron EDM or nuclear magnetic quadrupole moment, but in this Perspective we focus on the Schiff moment owing to the particular enhancement discussed shortly.

The nuclear Schiff moment is sensitive to the deviation of the nucleon positions from the mean-squared nuclear charge radius. The Schiff moment is given by[48]

$$\mathbf{S} = \mathbf{S}_{\mathrm{ch}} + \mathbf{S}_{\mathrm{n}} + \cdots = \sum_{i=1}^{A}\left(\frac{1}{10}\left(r_i^2 - \frac{5}{3}R_{\mathrm{ch}}^2\right)q_i\mathbf{r}_i + \frac{1}{6}(r_i^2 - R_{\mathrm{ch}}^2)\mathbf{d}_i\right) + \cdots, \quad (1)$$

in which $A = N + Z$ is the mass number, with N and Z the number of neutrons and protons, respectively, so that the sum is taken over all nucleons; i labels each nucleon, with r_i its position, q_i its electric charge and $\mathbf{d}_i$ its permanent EDM; R_{ch}^2 is the mean-squared nuclear charge radius and ... denotes higher-order contributions[47]. The charge term $\mathbf{S}_{\mathrm{ch}}$ receives direct contributions from the protons only, whereas the nucleon term $\mathbf{S}_{\mathrm{n}}$ contains contributions from permanent EDMs of individual nucleons. For large A, the term $\mathbf{S}_{\mathrm{ch}}$ is expected to dominate, as most nucleon spins are paired and do not contribute to the term $\mathbf{S}_{\mathrm{n}}$. Because $\mathbf{S}$ is a vector, by the Wigner–Eckart theorem the associated observable must lie along the nuclear spin $\langle \mathbf{S} \rangle \equiv S_z = \mathbf{S}\cdot\hat{z}_N \propto \langle \mathbf{S}\cdot\mathbf{I}\rangle$, in which $\hat{z}_N$ is along the quantization axis for the nuclear angular momentum $\mathbf{I}$. At the same time, such a correlation of a P-odd vector $\mathbf{S}$ with a T-odd spin $\mathbf{I}$ can only exist if there is P and T violation, equivalent to CPV, in the nuclear Hamiltonian. Indeed, S_z can be expanded in perturbation theory as:

$$S_z = \sum_e \frac{\langle g|\mathbf{S}|e\rangle\langle e|H_{\mathrm{CPV}}|g\rangle}{E_g - E_e} + c.c., \quad (2)$$

in which the sum is taken over opposite-parity excited states $|e\rangle$ with energy E_e. Here, H_{CPV} is the CP violating portion of the nuclear Hamiltonian[16,49], discussed further in the next section. The H_{CPV} interaction slightly polarizes the ground state $|g\rangle$ by mixing the opposite-parity excited nuclear states, causing a CP-odd orientation of the intrinsic Schiff moment, collinear with $\mathbf{I}$, which can be observed in the laboratory frame. Owing to both the near cancellation of terms in equation (1) and the sum over nuclear excited states in equation (2), nuclear theory calculations of Schiff moments require state-of-the-art methods[48,50,51].

The sensitivity of nuclear Schiff moments to new physics is markedly enhanced in certain nuclei that exhibit static octupole shape deformation ($|\beta_3| > 0$)[16,41,48,50,52,53]. The rotational states of such nuclei are described by symmetric top wavefunctions $|I, K\rangle$, with $K = \mathbf{I}\cdot\hat{z}_N$, which split into nearly-degenerate parity doublet states, $|\pm\rangle \propto |I,K\rangle \pm |I,-K\rangle$, similar to the description of nearly degenerate, opposite-parity molecular states[54,55]. The enhancement of the Schiff moment arises from two key features in the perturbative expression of equation (2): the large intrinsic Schiff moment $\langle I,K|\mathbf{S}|I,K\rangle$ in the body-fixed (intrinsic) frame owing to collective effects, and the small energy splitting between opposite-parity states, for instance, $\Delta E_\pm \approx 50$ keV in octupole-deformed ^{225}Ra (ref. 54). Such parity doublets allow for the unique perturber approximation, reducing the sum over $|e\rangle$ in equation (2) to a single opposite-parity excited state, simplifying calculations. The expression for S_z in octupole-deformed nuclei is then approximately[46,52]

$$S_z \approx 2\frac{\langle +|\mathbf{S}|-\rangle\langle -|H_{\mathrm{CPV}}|+\rangle}{\Delta E_\pm} \propto \frac{\beta_2\beta_3^2 Z A^{2/3}}{\Delta E_\pm}, \quad (3)$$

where we have introduced the scaling of S_z derived from a particle-rotor approximation of H_{PT} in static octupole-deformed nuclei. Here, $\Delta E_\pm$ is the energy splitting between opposite-parity nuclear states, and β_2 and β_3 are the nuclear quadrupole and octupole deformation parameters, respectively[54]. The deformation parameters describe, in the intrinsic frame, the radius of the axially symmetric charge distribution as a function of the polar angle θ, given in terms of spherical harmonic functions by $R(\theta) = R_{\mathrm{ch}}(1 + \sum_\ell \beta_\ell Y_{\ell,0}(\theta,\phi))$.

From the scaling in equation (3), it can be seen that the Schiff moment is enhanced compared with spherical nuclei, such as ^{199}Hg, by a factor of $\mathcal{O}(1,000)$, with specific values depending on nuclear structure details[16,48,52]. In general, equation (3) is approximate; state-of-the-art calculations use EFTs to parameterize CPV interactions in the nucleus and then solve the many-body quantum problem with density functional theory techniques[50,51,53], with some recent progress also ongoing in lighter nuclei using ab initio nuclear theory[49,56,57]. Although we do not consider them further, we note that vibrationally octupole-deformed nuclei (with $\langle\beta_3\rangle = 0$ and $\langle\beta_3^2\rangle > 0$) can potentially exhibit Schiff enhancements due to octupole collectivity[52,58,59]. However, owing to the much larger parity splitting in these systems[55,60,61], the unique perturber approximation breaks down, resulting in order-of-magnitude theoretical uncertainties[59,62] that would benefit from further investigation.

Figure 1 provides an overview of nuclei exhibiting static quadrupole ($|\beta_2| > 0$) and octupole deformations ($|\beta_3| > 0$). Whereas quadrupole deformation is common in nuclei, octupole deformation occurs in specific places of the nuclear chart. In the nuclear shell model, octupole deformation originates from $r^3Y_{3,0}$ interactions between nuclear levels separated by $3\hbar$ of angular momentum near the Fermi surface[52,58,63]. Such interactions occur primarily in nuclei whose proton or neutron numbers (Z or N) are close to 34, 56, 88 or 134, just beyond spherical magic numbers[64]. The deformation is especially prominent in heavy, exotic nuclei near $Z \approx 88$ and $N \approx 134$ (such as isotopes of Fr, Ra, Ac, Th and Pa)[55]. However, the substantial nucleon imbalance in these isotopes renders them radioactive, typically limiting their lifetimes to a few days or less. Nonetheless, progress has been made in recent years on the production and spectroscopy of molecules containing octupole-deformed nuclei[37–39], providing unique opportunity for next-generation CPV searches.

Effective field theories and energy reach

To interpret searches for CPV moments as constraints on new physics, we must connect low-energy (less than gigaelectronvolts, 'IR') observables to their microscopic, high-energy (more than teraelectronvolts, 'UV') sources. This connection is made through a tower of EFTs that systematically bridge vastly different energy scales[11–14]. EFT approaches enable systematic, global analyses of CPV using EDM bounds from nucleons, atoms and molecules[65,66] as well as combined analyses with collider experiments[35,67,68]. Two key EFT frameworks are the standard model EFT (SMEFT)[14,69] in high-energy physics and chiral EFT (χEFT)[13,48,49] in nuclear physics. SMEFT describes how generic new particles and forces at more than teraelectronvolt energies modify interactions of standard model fields at and below the electroweak scale (approximately less than or equal to teraelectronvolts), whereas χEFT describes low-energy, non-perturbative QCD at less than gigaelectronvolt energies in terms of composite nucleons and pions. A schematic overview of EFT sources of molecular CPV is shown in Fig. 2.

Although EFTs provide a systematic framework for connecting CP-violating observables to microscopic sources of new physics, they represent only one layer in the full theoretical interpretation chain relevant for radioactive molecule experiments. On the low-energy side,

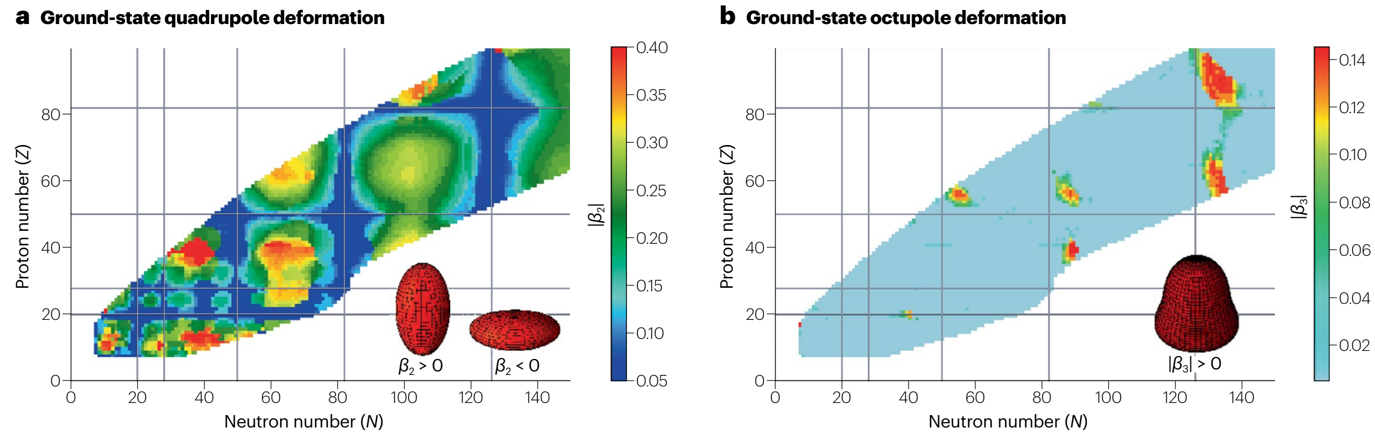

Fig. 1 | Quadrupole and octupole deformation across the nuclear chart. The parameters β_2 and β_3 characterize deviations of a nucleus from spherical symmetry. **a**, The quadrupole deformation parameter β_2 corresponds to elongated (prolate) or flattened (oblate) shapes, respectively. **b**, The octupole deformation parameter β_3 describes pear-like shapes that do not exhibit reflection symmetry. Data replotted from ref. 142. Figure courtesy of Jose Miguel Munoz Arias.

χEFT interactions must be embedded in realistic nuclear many-body calculations to determine nuclear moments such as Schiff moments, particularly in heavy, octupole-deformed nuclei. In parallel, relativistic atomic and molecular structure calculations are required to translate these nuclear moments into experimentally observable energy shifts, through the determination of electronic enhancement factors and internal effective fields.

In practice, estimates of experimental sensitivity for a given radioactive molecule rely on the combined input of EFT matching, nuclear structure theory and molecular electronic structure calculations, often well in advance of experimental measurements. Continued progress across all three areas is therefore essential for both the interpretation and design of next-generation searches for CPV. For heavy nuclei, state-of-the-art calculations use nuclear density functional theory[50,51], and ab initio approaches remain limited to lighter systems[57,70,71]. At the molecular level, relativistic many-electron calculations determine the electronic enhancement factors and internal effective fields that convert a given Schiff moment into a measurable frequency shift. After parameterizing nuclear Schiff moments in terms of χEFT and SMEFT coefficients, SMEFT can be used to estimate the energy reach of hadronic EDM experiments. Owing to the large number of CPV operators that couple to quarks and gluons, hadronic EDM searches probe a broader region of SMEFT parameter space than purely leptonic measurements do.

Using dimensional analysis arguments, we can estimate the energy reach of hadronic EDM measurements with radioactive molecules containing octupole-deformed nuclei. For simplicity, we focus on the fermionic EDMs and chromo-EDMs, which can be estimated as[5,17,32]:

$$d_\mathrm{f} \sim q_\mathrm{f} \sin\phi_\mathrm{CP} \left(\frac{g^2}{16\pi^2}\right)^{\ell} \frac{m_\mathrm{f}}{\Lambda_\mathrm{NP}^2}, \qquad (4)$$

in which q_f and m_f are the fermion's (colour) charge and mass, respectively, ϕ_CP is the CP-violating phase characterizing the complex Wilson coefficient (the contribution to the CP-even magnetic dipole is scaled by $\cos\phi_\mathrm{CP}$), ℓ is the number of loops in the Feynman diagram that gives rise to the EDM and g is the strength of the coupling constants in the loop. Loops involving standard model interactions receive factors of $g_\mathrm{EM} \sim 0.3$, $g_\mathrm{W} \sim 0.6$, $g_\mathrm{S} \sim 1$ and typically $\sin(\phi_\mathrm{CP})$ and g_BSM are taken to be $\mathcal{O}(1)$ quantities without additional fine-tuning. Tree-level ($\ell = 0$) diagrams have the highest energy reach but are sensitive to only a few beyond-standard model interactions, whereas one-loop and two-loop ($\ell = 1$ and $\ell = 2$) diagrams incorporate wider operator reach at the cost of $\mathcal{O}(10^2)$ to $\mathcal{O}(10^4)$ loop suppression. Although two-loop bounds generically have suppressed energy reach compared with one-loop bounds, two-loop processes can be enhanced by heavy quark contributions and renormalization mixing, relevant for constraining various new physics scenarios[15,32,33].

Figure 3 illustrates the one-loop energy reach probing Λ_NP and the value of $\bar{\theta}$ constrained by prior hadronic EDM measurements using systems such as the neutron, atomic Hg, Xe and Ra and molecular TlF. The leading bounds on hadronic CPV arise from EDM measurements of the neutron[22] and Hg atom[72], already probing energy scales on the order of 10 TeV in the single-source approximation. Comparison with the potential reach of radioactive molecules can be made by calculating the EDM limit assuming measurements at the standard quantum limit (SQL)[17]:

$$\delta d_\mathrm{f} \simeq \underbrace{\frac{\hbar}{\tau\sqrt{NRT}}}_{\text{SQL}} \times \underbrace{\frac{1}{\langle I_z\rangle W_\mathrm{S}}}_{\text{Molecular}} \times \underbrace{\frac{1}{S_z(\bar{g}_0(\bar{\theta}\ldots), \bar{g}_1(\tilde{d}_1\ldots), \ldots)}}_{\text{Nuclear}}, \qquad (5)$$

in which the first factor describes the SQL obtained from Ramsey measurements, given a coherence time τ and NRT detected molecules, with N molecules per experiment cycle, R the cycle repetition rate and T the total experiment run-time. (Note that when the repetition rate is limited by the coherence time, that is, $R_\mathrm{p} \propto \tau^{-1}$, the coherence time scaling is reduced to $\delta d_\mathrm{f} \propto \tau^{-1/2}$). The molecular enhancement term is given by the product of the polarization of nuclear spin along the internal molecular axis, $\langle I_z\rangle$, and the calculated electronic enhancement factor, W_S, describing the internal molecular fields near the nucleus[73]. Finally, the nuclear enhancement term (as discussed in the previous section) describes the scaling of the Schiff moment in terms of the underlying low-energy constants (LECs), which can then be related to underlying Wilson coefficients.

Figure 3 shows the potential constraints that could be set using molecules with octupole-deformed nuclei, labelled by number of molecules per experiment cycle, coherence time and total measurement duration. For reference, state-of-the-art trapped molecule experiments have achieved >10^4 laser-cooled CaF molecules in a conservative optical trap at 14 μK (ref. 74) and second-scale coherence in optically trapped, ultracold RbCs molecules. Importantly, there is a pathway to further improve bounds using the toolbox of

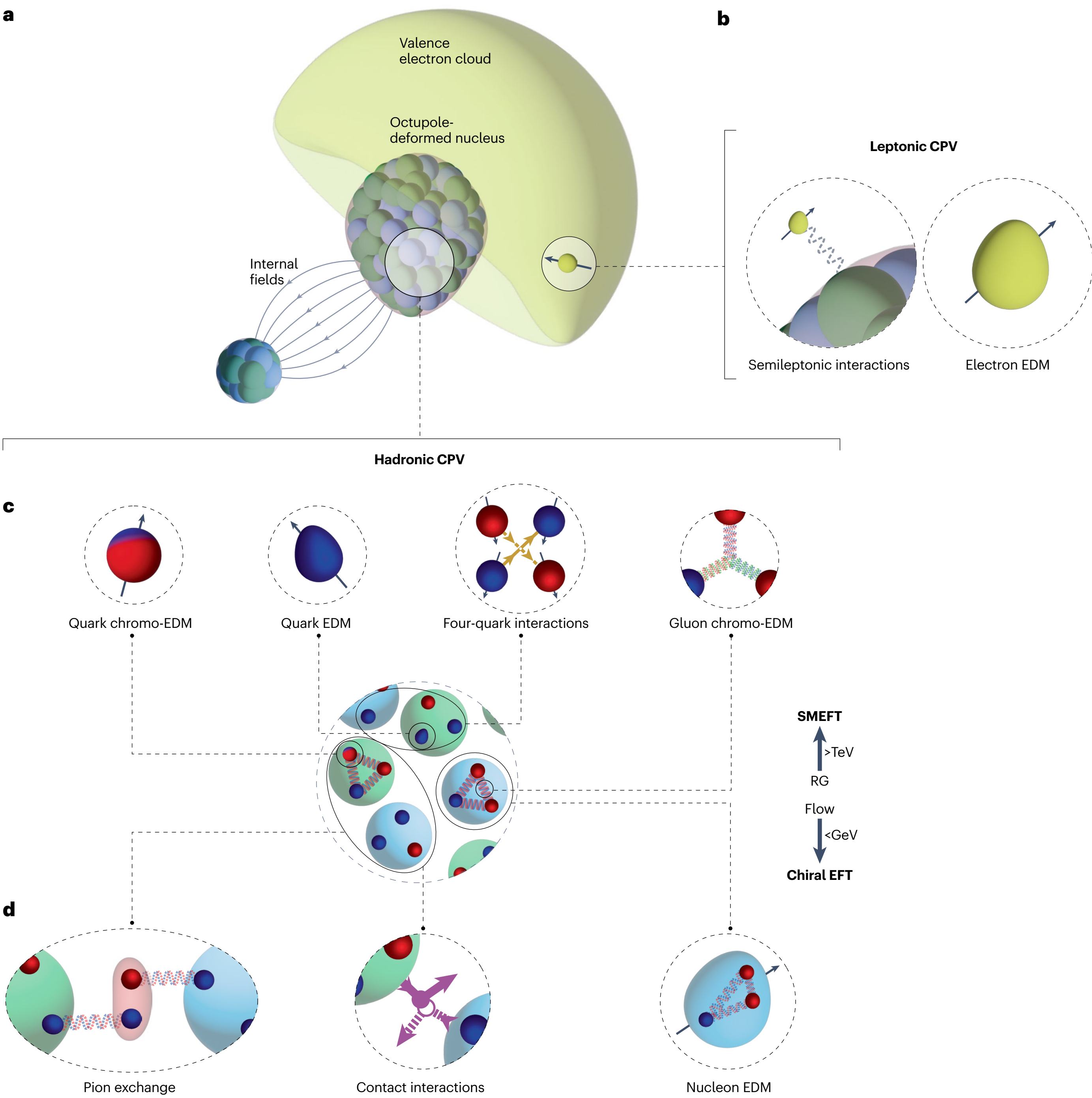

Fig. 2 | Sources of CP violation among the constituents of a diatomic molecule. a, Schematic representation of a diatomic molecule containing an octupole-deformed nucleus and large external fields. **b**, Electrons interact with the nucleus primarily via electromagnetic and weak forces, and electron electric dipole moment (EDM) experiments primarily probe leptonic charge–parity violation (CPV). Inside nuclei, additional complex interactions occur among protons and neutrons, as well as their fundamental building blocks – quarks and gluons – through a combination of the electromagnetic, weak and strong forces. At high energies (part **c**), these microscopic quantum chromodynamics sources of CPV are captured by the standard model effective field theory (SMEFT) and connected via renormalization group (RG) flow to low-energy, less than gigaelectronvolt chiral EFT interactions (part **d**). The octupole deformation of the nucleus and the large internal fields in the molecule provide enhanced sensitivity to several sources of hadronic CPV, most prominently CPV pion exchange[28,38].

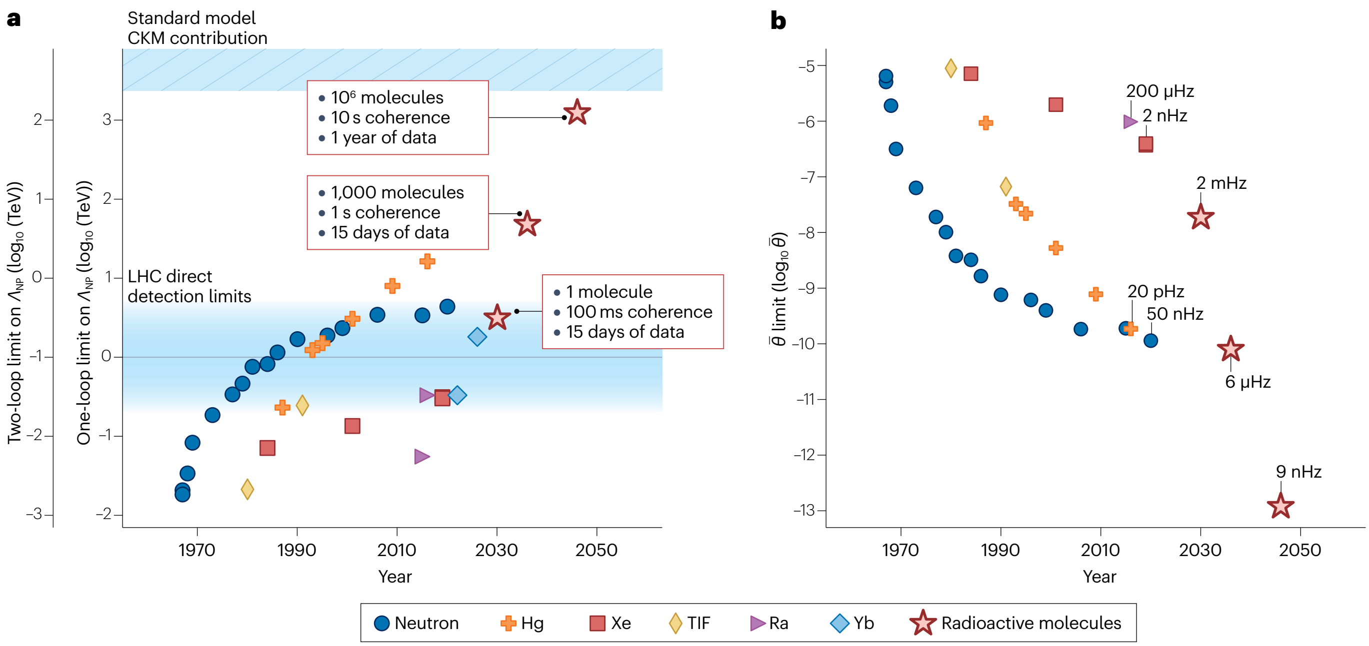

Fig. 3 | Hadronic electric dipole moment limits. Prospects for probing new physics with radioactive molecules (pink stars), in comparison to current Large Hadron Collider (LHC) limits (horizontal faded band) and previous hadronic electric dipole moment measurements. Hadronic enhancement factors from equation (2) in the Supplementary information are estimated by geometric means of the values in ref. 48. **a**, One-loop and two-loop limits on the new physics energy scale, Λ_{NP}, obtained from a single-source approximation of $\bar{g}_0$ from an isovector quark chromoelectric-EDM (CEDM) $\tilde{d}_1$. See ref. 17 for more details. LHC constraints taken from refs. 143–145. The equivalent signal from the standard model Cabibbo–Kobayashi–Maskawa (CKM) contribution is shown with the hatched region. **b**, Limits on $\bar{\theta}$ from a single-source approximation considering only CPV pion exchange $\bar{g}_0$. The best limits from ^{225}Ra, ^{129}Xe, ^{199}Hg, ^{171}Yb, and the neutron, as well as radioactive molecule projections, are labelled with their frequency precision, contextualizing differences in sensitivity. For $\bar{\theta}$, both the expected standard model CKM contribution[5,19] at $\bar{\theta} \sim 10^{-16}$ and the quantum chromodynamics axion oscillation scale[26] at $\bar{\theta}_{rms} \sim 4 \times 10^{-19}$ lie outside the plotted range. All calculations assume 1 s experimental cycle dead-time. Compiled measurements and constraints are available at ref. 146.

molecular quantum control[28,29]. Advanced measurements with radioactive molecules could potentially achieve constraints beyond the 1,000 TeV scale, thereby covering the discovery window between the limits set by direct searches at the LHC and the known sources of CPV within the standard model. The parameters required to reach the standard model contribution have already been demonstrated in state-of-the-art experiments with cold, stable atoms and molecules[4,29]; applying these techniques to radioactive molecules promises to have a significant impact on searches for new symmetry-violating physics.

Experimental techniques and challenges

Radioactive molecules containing octupole-deformed nuclei are often produced in extremely trace quantities and are typically reactive or refractory. As a result, major challenges stand in the way of precision measurement with these molecules. Experiments with radioactive material require special consideration in storage, handling, disposal and experimental design. Their scarcity also requires highly efficient chemistry, trapping, spectroscopy and measurement techniques, at a level not previously necessary for stable species.

Production of radioactive isotopes

The growing interest in studying unstable nuclei for both foundational physics and practical applications has driven the development of numerous major radioactive beam facilities worldwide[75], such as FRIB at MSU (USA), ISOLDE at CERN (Europe), RIBF at RIKEN (Japan) and ISAC at TRIUMF (Canada). Experimental programmes focused on radioactive molecules are being developed at these facilities and are expected to be operational in the coming decade[38]. These facilities use various nuclear reactions to produce and efficiently extract isotopes of interest in both atomic and molecular forms. ISOLDE and TRIUMF provide chemically separated, high-purity atomic and molecular beams, whereas FRIB generates a broader range of exotic nuclei through in-flight fragmentation[76]. The latter is more suitable for refractory elements such as Th and Pa, both of special interest for symmetry-violation searches. A new isotope-harvesting initiative at FRIB[77] aims to provide access to short-lived and long-lived radioisotopes, such as ^{225}Ra, ^{225}Ac and ^{229}Th, which could serve as valuable sources of rare isotopes without requiring dedicated beam time. Harvested isotopes of interest can be purified and transported for precision experiments and rapid prototyping at university laboratories.

In addition to beam facilities, major nuclear physics laboratories, such as ORNL[78,79] (USA), specialize in the production and separation of actinide and transuranium nuclei, to facilitate construction of offline sources. For instance, experiments in laser cooling and trapping[80] atomic ^{221}Fr and ^{225}Ra used sources with the parent isotopes ^{225}Ac and ^{229}Th, respectively[81,82]. In these sources, the daughter products are collected either via evaporation of the daughter through heating or via α-decay recoil, which ejects the daughters from the surface of the sample. Offline sources typically provide less instantaneous flux than dedicated facilities, but in many cases they offer a complementary alternative compared with the costs and scheduling limitations of facility beam time. Additionally, for species with long-lived parent isotopes, offline sources can operate for years to decades without need for renewal. Overall, offline sources can provide a flexible, potentially long-term solution that enables various experiments at university laboratories. Mature experiments can then be adapted to perform online measurement runs at beam facilities, taking advantage of high-flux radioisotope production and advanced radioactive material-handling capabilities.

Spectroscopy

Precision spectroscopy of short-lived radioactive molecules has become possible in the past few years owing to the development of highly sensitive production and detection schemes[37]. Starting with the production of radioactive molecular ions RaF^+, followed by their subsequent neutralization into RaF, overall efficiency of more than 10% has been demonstrated, with molecular fluxes on the order of 10^7 molecules per second[37,83], enabling studies of the short-range electron–nucleus interactions[84] and providing an experimental determination of a laser-cooling scheme for RaF[85–87]. This progress has motivated the emergence of a new research area at laboratories across Europe and North America[38], with experiments already extended to other actinide molecules such as AcF[88]. However, these experiments were performed using a hot, energetic beam of molecules, with kinetic energies of ~40 keV and internal temperatures exceeding 1,000 K. A primary challenge lies in the efficient production of slow, cold radioactive molecules with subkelvin temperatures, which are essential for further precision experiments and for enabling efficient laser-cooling techniques. Production and spectroscopy of cold ^{226}RaOH, ^{226}RaOD and ^{226}RaF were recently demonstrated via cryogenic buffer gas cooling[89] and laser-driven chemistry[90], with yields of up to ~10^{10} molecules per pulse at temperatures between 4 K and 7 K (ref. 39).

Deceleration and cooling

Measurements with cold beams of molecules are a demonstrated method for performing spectroscopy with kilohertz or better resolution, as well as precision measurements of fundamental symmetries with less than millihertz precision. The ACME (Advanced Cold Molecule Electron EDM) experiment, for example, has used a cold beam of neutral ThO molecules to set limits on the EDM of an electron[31]. To realize maximum sensitivity, these beam sources must be cold, slow and bright. A temperature of $\lesssim$10 K ensures that a relatively small number of internal states are populated, concentrating population in the lowest rotational and hyperfine quantum states. High brightness (flux per unit solid angle per second) ensures high counting statistics. Low forward velocity not only increases interaction time while maintaining a short beam line but also enables slowing and cooling into a trap. For neutral molecules, the leading approach is the cryogenic buffer gas beam[89], which can be used to create cold, slow and bright beams of essentially any species, including those which are reactive or refractory. Molecular beams can be produced directly in a cryogenic buffer gas cell by laser ablation of a precursor in the presence of buffer gas, which can also be combined with reagent gas flowed in via a heated capillary[89]. Alternatively, cryogenic buffer gas cells can be used to slow initially hot and fast beams. This approach has been used to produce cryogenic beams of atoms loaded from thermal ovens[91] and also used at radioactive ion beam facilities to stop gigaelectronvolt beams[92,93]. Neutral radium-containing species, which have been recently cooled in a cryogenic buffer gas cell[39], are currently being pursued for laser cooling and trapping[94,95].

Ion trapping

Ion traps are well suited to working with radioactive atomic and molecular species[96]. Strong electromagnetic control relaxes requirements on low beam velocity, enabling rapid prototyping and production of free radicals using supersonic expansion cooling[89]. Furthermore, ion traps are deep, which make it routine to hold particles continuously for months (or until they decay)[97]. The trapping mechanism depends only on the charge and mass of the molecule, making ion traps agnostic at first order to complex internal molecular structure[98]. Additionally, higher-order sensitivities can provide an avenue for readout via Stern–Gerlach-like effects[99]. In addition to the long hold times, ion traps may be used to efficiently work with a few particles, often realizing precision measurements with only a single trapped ion[100].

Because ion traps are insensitive to internal structure, it is straightforward to simultaneously hold different elements in the same trapping potential, as long as the charge-to-mass ratios are not too different. Co-trapping laser-coolable atoms with molecular ions provides opportunities for controlling the molecules with the atoms via the shared motional modes of the ion trap. An early realization[101] that leveraged these strengths was quantum logic spectroscopy (QLS) of Al^+ with co-trapped Be^+. In this experiment, Be^+ cooled a motional mode of the ion pair to the ground state and then was used to perform high fidelity readout of Al^+ after it was probed with a spectroscopy pulse. QLS was developed because Al^+, like molecules, does not have good cycling transitions, and therefore this approach could also be used for molecular spectroscopy[101]. This led to QLS state detection of a molecule[102], followed by state detection and state preparation of a molecule[103], and subsequent advances in controlling molecule rotational states[104]. QLS could provide a means to very efficiently use a single particle (or few particles) that may be challenging to produce in large quantities, especially helpful for trace radioactive species. Other efficient spectroscopy techniques have recently been developed that could be applied to polyatomic radioactive molecules[105].

Advances in Paul ion trap technology have been driven by both quantum information science[106,107] and precision measurement[108] and have included world-record electron EDM measurements using HfF^+ (refs. 28,30). These advances could be combined with emerging techniques, such as QLS, with many trapped radioactive molecules. Precision science using heavy molecular ions with small rotational constants will likely require cryogenic systems to reduce population scrambling by blackbody radiation. Cryogenic ion traps are increasingly used owing to advantages such as their very low pressures[109]. For EDM searches, molecules must be polarized with an electric field, but the molecular ions should not be pushed by the field out of the locations where they are polarized. This challenge has been addressed with rotating electric fields[30], but there are opportunities to use other dynamic schemes[110,111]. The demonstration of QLS and coherent state control with CaH^+ molecular ions[104] offers a compelling route for precision measurements with molecular ions such as $RaOH^+$ or $RaOCH_3^+$ (refs. 112–114) or polycations such as PaF^{3+} (ref. 115), in which the long-lived electronic states provide natural shielding from blackbody radiation. Penning ion traps are also intriguing for their use with radioactive molecules. They have been used extensively with radioactive species[96] and for precision measurements[116]. In part owing to their large magnetic field, Penning traps have been recently considered for measuring parity violation with radioactive molecules[117].

Laser cooling and trapping

A major area of current work is performing laser cooling and trapping of molecules sensitive to fundamental symmetries, including radioactive molecules[38]. Ultracold and trapped neutral species offer a pathway to large numbers, long coherence times and extreme levels of control, and in recent years these have been important drivers behind advances in ultracold atom and molecule science. However, direct laser cooling of molecules is an active area of research[29], and extending these techniques to radioactive molecules remains one of the major current challenges in the field.

Direct laser cooling of molecules has progressed since it was demonstrated experimentally in 2010 (ref. 118). Advances include optical dipole trapping, magnetic trapping, tweezer trapping, controlled interactions, quantum gates and quantum control for fundamental symmetry-violation searches[29,94,95]. Molecules that can be laser-cooled using known methods are relatively uncommon, but radium-containing species such as RaF[37,85,119] and RaOH[120,121] are predicted to be laser-coolable, thereby offering a potential route towards integrating state-of-the-art quantum methods with radioactive nuclei bound in molecules.

Current efforts with stable molecules have pushed the frontier of laser cooling and quantum control for complex molecules. The laser cooling of triatomic species such as CaOH[43] and SrOH[122], which offers better polarizability and systematic corrections compared with diatomics[112], has opened exciting prospects for symmetry tests with radioactive analogues such as RaOH[112,120].

Assembling molecules

In addition to direct laser cooling, radioactive molecules could potentially be assembled from laser-cooled atoms. This approach has been successful in ultracold bi-alkali molecules[123], although these molecules tend to have low sensitivity to fundamental symmetry violation[124], even if one of the species is heavy such as Fr or Ra. However, bonding heavy alkali or alkaline-earth atoms with Ag results in a large molecular enhancement of CPV sensitivity[125–128], and experiments are currently under development[129] to produce ultracold ^{223}FrAg. Likewise, optical tweezer arrays have emerged as a tool for assembling individual molecules from ultracold atoms[130,131] and may provide a route to create ultracold, radioactive molecules from trace samples of radioactive atoms.

Solid-state systems

Additional promising directions involve the use of noble gas solids to trap and orient molecules[132] and atomic ions embedded in optical crystals[133,134] or diamonds[135] where they are exposed to large local electric fields. These solid-state systems can accommodate number densities as high as 10^{15} cm^{-3}, far exceeding those of conventional laser and ion traps, while remaining sufficiently dilute to allow nuclear spin coherence times on the order of a second or longer[136,137]. In a suitably chosen host solid, as pointed out in the 1960s in the context of paramagnetic ions in corundum[138], the guest species occupies pairs of trapping sites where the effective internal electric field felt by the nucleus is equal in magnitude but opposite in orientation[139], making the rejection of common mode systematic effects feasible. Matrix isolation techniques, in which molecules are trapped in inert gas solids, offer a unique platform for precision spectroscopy and quantum control[132]. The ability to efficiently use small samples, the prospect of oriented molecules in the matrix and the long coherence times could be particularly advantageous for experiments with rare radioactive species.

Outlook

In addition to searches for CPV, precision studies of radioactive molecules are of interest across multiple subfields in physics and chemistry[38]. Measurements of isotope shifts and hyperfine structure can probe nuclear size variations and electromagnetic moments in nuclear matter far from equilibrium. Although the vast majority of such experiments have been conducted using radioactive atoms[140], extending them to radioactive molecules is of interest because molecules can offer enhanced sensitivity for studying nuclear electroweak properties[117] and are important in astrophysics[38]. Radioactive molecule spectroscopy is particularly useful to study elements that preferentially form molecules, or in cases in which atomic states have angular momentum structure that is insensitive to nuclear moments. Moreover, laboratory spectra of complex radioactive molecules are essential for unambiguously identifying such species in astrophysical environments, where they can be naturally produced[141].

There are also opportunities to further develop radioactive molecular techniques and expand the range of systems being studied. Improvements in molecular beam intensity, laser cooling and ion trapping will enable experiments with even rarer molecular species. Furthermore, the integration of new approaches – such as isotope harvesting, quantum-enhanced sensing and matrix isolation – is key to unlocking the full potential of radioactive molecules. As these techniques mature and are combined in new ways, they will enable a range of precision measurements with octupole-deformed nuclei. With unprecedented sensitivity to fundamental symmetry violation, radioactive molecules can fully cover the discovery window (Fig. 3), with the potential to unveil new sources of CP violation, shed light on the strong CP problem and probe physics at the petaelectronvolt scale.

Realizing this scientific potential will require a concerted effort that cuts across traditional disciplinary boundaries. Success will be enabled by experimental advances in rare isotope production at accelerator facilities, laser cooling and molecular beam techniques, ion trapping and quantum control, and ultracold assembly of molecules, with these efforts matched by progress in relativistic many-body theory, nuclear structure models and particle physics calculations. The multifaceted nature of these challenges presents opportunities for cross-community collaboration and interdisciplinary innovation.

Published online: 22 June 2026

References

1. Aaij, R. et al. Measurement of matter–antimatter differences in beauty baryon decays. *Nat. Phys.* **13**, 391–396 (2017).
2. Bar-Shalom, S., Soni, A. & Wudka, J. Theoretical underpinnings of CP-violation at the high-energy frontier. *Phys. Lett. B* **860**, 139135 (2025).
3. Artuso, M. et al. Report of the frontier for rare processes and precision measurements. Preprint at https://arxiv.org/abs/2210.04765 (2022).
4. Safronova, M. S. et al. Search for new physics with atoms and molecules. *Rev. Mod. Phys.* **90**, 025008 (2018).
5. Chupp, T. E., Fierlinger, P., Ramsey-Musolf, M. J. & Singh, J. T. Electric dipole moments of atoms, molecules, nuclei, and particles. *Rev. Mod. Phys.* **91**, 015001 (2019).
6. Canetti, L., Drewes, M. & Shaposhnikov, M. Matter and antimatter in the universe. *New J. Phys.* **14**, 095012 (2012).
7. Sakharov, A. D. Violation of CP invariance, C asymmetry, and baryon asymmetry of the universe. *JETP Lett.* **5**, 24–27 (1967).
8. de Vries, J., Postma, M., van de Vis, J. & White, G. Electroweak baryogenesis and the standard model effective field theory. *J. High Energy Phys.* **2018**, 89 (2018).
9. Isidori, G. & Straub, D. M. Minimal flavour violation and beyond. *Eur. Phys. J. C* **72**, 1–14 (2012).
10. Greljo, A., Palavrić, A. & Thomsen, A. E. Adding flavor to the SMEFT. *J. High Energy Phys.* **2022**, 10 (2022).
11. Georgi, H. Effective field theory. *Annu. Rev. Nucl. Part. Sci.* **43**, 209–252 (1993).

12. Manohar, A. V. in *Effective Field Theory in Particle Physics and Cosmology: Lecture Notes of the Les Houches Summer School* Vol. 108 (eds Davidson, S. et al.) 47–136 (Oxford Univ. Press, 2020).
13. Hammer, H.-W., König, S. & Van Kolck, U. Nuclear effective field theory: status and perspectives. *Rev. Mod. Phys.* **92**, 025004 (2020).
14. Isidori, G., Wilsch, F. & Wyler, D. The Standard Model effective field theory at work. *Rev. Mod. Phys.* **96**, 015006 (2024).
15. Pospelov, M. & Ritz, A. Electric dipole moments as probes of new physics. *Ann. Phys.* **318**, 119–169 (2005).
16. Engel, J., Ramsey-Musolf, M. J. & Van Kolck, U. Electric dipole moments of nucleons, nuclei, and atoms: the Standard Model and beyond. *Prog. Part. Nucl. Phys.* **71**, 21–74 (2013).
17. Alarcon, R. et al. Electric dipole moments and the search for new physics. Preprint at https://arxiv.org/abs/2203.08103 (2022).
18. Seng, C.-Y. Reexamination of the standard model nucleon electric dipole moment. *Phys. Rev. C* **91**, 025502 (2015).
19. Dragos, J., Luu, T., Shindler, A., de Vries, J. & Yousif, A. Confirming the existence of the strong CP problem in lattice QCD with the gradient flow. *Phys. Rev. C* **103**, 015202 (2021).
20. Ema, Y., Gao, T. & Pospelov, M. Standard model prediction for paramagnetic electric dipole moments. *Phys. Rev. Lett.* **129**, 231801 (2022).
21. Hook, A. TASI lectures on the strong CP problem and axions. Preprint at https://arxiv.org/abs/1812.02669 (2018).
22. Abel, C. et al. Measurement of the permanent electric dipole moment of the neutron. *Phys. Rev. Lett.* **124**, 081803 (2020).
23. De Vries, J., Draper, P., Fuyuto, K., Kozaczuk, J. & Sutherland, D. Indirect signs of the Peccei–Quinn mechanism. *Phys. Rev. D* **99**, 015042 (2019).
24. Peccei, R. D. & Quinn, H. R. CP conservation in the presence of pseudoparticles. *Phys. Rev. Lett.* **38**, 1440–1443 (1977).
25. Kim, J. E. & Carosi, G. Axions and the strong CP problem. *Rev. Mod. Phys.* **82**, 557–601 (2010).
26. de Vries, J., Draper, P., Fuyuto, K., Kozaczuk, J. & Lillard, B. Uncovering an axion mechanism with the EDM portfolio. *Phys. Rev. D* **104**, 055039 (2021).
27. Adams, C. et al. Axion dark matter. Preprint at https://arxiv.org/abs/2203.14923 (2022).
28. Cairncross, W. B. & Ye, J. Atoms and molecules in the search for time-reversal symmetry violation. *Nat. Rev. Phys.* **1**, 510–521 (2019).
29. DeMille, D., Hutzler, N. R., Rey, A. M. & Zelevinsky, T. Quantum sensing and metrology for fundamental physics with molecules. *Nat. Phys.* **20**, 741–749 (2024).
30. Roussy, T. S. et al. An improved bound on the electron's electric dipole moment. *Science* **381**, 46–50 (2023).
31. Andreev, V. et al. Improved limit on the electric dipole moment of the electron. *Nature* **562**, 355–360 (2018).
32. Cesarotti, C., Lu, Q., Nakai, Y., Parikh, A. & Reece, M. Interpreting the electron EDM constraint. *J. High Energy Phys.* **2019**, 59 (2019).
33. Panico, G., Pomarol, A. & Riembau, M. EFT approach to the electron electric dipole moment at the two-loop level. *J. High Energy Phys.* **2019**, 090 (2019).
34. Brod, J. & Stamou, E. Electric dipole moment constraints on CP-violating heavy-quark Yukawas at next-to-leading order. *J. High Energy Phys.* **2021**, 80 (2021).
35. Bahl, H. et al. Constraining the CP structure of Higgs-fermion couplings with a global LHC fit, the electron EDM and baryogenesis. *Eur. Phys. J. C* **82**, 604 (2022).
36. Kley, J., Theil, T., Venturini, E. & Weiler, A. Electric dipole moments at one-loop in the dimension-6 SMEFT. *Eur. Phys. J. C* **82**, 1–43 (2022).
37. Garcia Ruiz, R. F. et al. Spectroscopy of short-lived radioactive molecules. *Nature* **581**, 396–400 (2020).
38. Arrowsmith-Kron, G. et al. Opportunities for fundamental physics research with radioactive molecules. *Rep. Prog. Phys.* **87**, 084301 (2024).
39. Conn, C. J. et al. Production and spectroscopy of cold radioactive molecules. Preprint at https://arxiv.org/abs/2508.08368 (2025).
40. Gaffney, L. P. et al. Studies of pear-shaped nuclei using accelerated radioactive beams. *Nature* **497**, 199–204 (2013).
41. Auerbach, N., Flambaum, V. V. & Spevak, V. Collective T- and P-odd electromagnetic moments in nuclei with octupole deformations. *Phys. Rev. Lett.* **76**, 4316–4319 (1996).
42. Hutzler, N. R. Polyatomic molecules as quantum sensors for fundamental physics. *Quantum Sci. Technol.* **5**, 044011 (2020).
43. Anderegg, L. et al. Quantum control of trapped polyatomic molecules for eEDM searches. *Science* **382**, 665–668 (2023).
44. Takahashi, Y. et al. Engineered molecular clock transitions for symmetry violation searches. Preprint at https://arxiv.org/abs/2508.06787 (2025).
45. Schiff, L. I. Measurability of nuclear electric dipole moments. *Phys. Rev.* **132**, 2194 (1963).
46. Flambaum, V. & Ginges, J. Nuclear Schiff moment and time-invariance violation in atoms. *Phys. Rev. A* **65**, 032113 (2002).
47. Liu, C.-P. P., Ramsey-Musolf, M. J., Haxton, W. C., Timmermans, R. G. E. & Dieperink, A. E. L. Atomic electric dipole moments: the Schiff theorem and its corrections. *Phys. Rev. C* **76**, 035503 (2007).
48. Engel, J. Nuclear Schiff moments and CP violation. *Annu. Rev. Nucl. Part. Sci.* **75**, 129–151 (2025).
49. De Vries, J. et al. Parity-and time-reversal-violating nuclear forces. *Front. Phys.* **8**, 218 (2020).
50. Dobaczewski, J., Engel, J., Kortelainen, M. & Becker, P. Correlating Schiff moments in the light actinides with octupole moments. *Phys. Rev. Lett.* **121**, 232501 (2018).
51. Zhou, E., Yao, J., Engel, J. & Meng, J. Effects of beyond-mean-field correlations on nuclear Schiff moments. Preprint at https://arxiv.org/abs/2507.01369 (2025).
52. Engel, J., Friar, J. L. & Hayes, A. C. Nuclear octupole correlations and the enhancement of atomic time-reversal violation. *Phys. Rev. C* **61**, 035502 (2000).
53. Dobaczewski, J. & Engel, J. Nuclear time-reversal violation and the Schiff moment of ^{225}Ra. *Phys. Rev. Lett.* **94**, 232502 (2005).
54. Butler, P. A. & Nazarewicz, W. Intrinsic reflection asymmetry in atomic nuclei. *Rev. Mod. Phys.* **68**, 349–421 (1996).
55. Butler, P. A. Pear-shaped atomic nuclei. *Proc. R. Soc. A Math. Phys. Eng. Sci.* **476**, 20200202 (2020).
56. Gnech, A., De Vries, J., Shain, S. & Viviani, M. Electric dipole moment of light nuclei in chiral effective field theory. *EPJ Web Conf.* **258**, 06007 (2022).
57. Hergert, H. A guided tour of ab initio nuclear many-body theory. *Front. Phys.* **8**, 379 (2020).
58. Butler, P. A. Octupole collectivity in nuclei. *J. Phys. G Nucl. Part. Phys.* **43**, 073002 (2016).
59. Flambaum, V. & Feldmeier, H. Enhanced nuclear Schiff moment in stable and metastable nuclei. *Phys. Rev. C* **101**, 015502 (2020).
60. Butler, P. A. et al. The observation of vibrating pear-shapes in radon nuclei. *Nat. Commun.* **10**, 2473 (2019).
61. Butler, P. A. et al. Evolution of octupole deformation in radium nuclei from Coulomb excitation of radioactive ^{222}Ra and ^{228}Ra beams. *Phys. Rev. Lett.* **124**, 042503 (2020).
62. Sushkov, O. P. Schiff moments of deformed nuclei. *Phys. Rev. C* **110**, 015501 (2024).
63. Chen, M., Li, T., Dobaczewski, J. & Nazarewicz, W. Microscopic origin of reflection-asymmetric nuclear shapes. *Phys. Rev. C* **103**, 034303 (2021).
64. Cao, Y., Agbemava, S. E., Afanasjev, A. V., Nazarewicz, W. & Olsen, E. Landscape of pear-shaped even-even nuclei. *Phys. Rev. C* **102**, 024311 (2020).
65. Degenkolb, S., Elmer, N., Modak, T., Mühlleitner, M. & Plehn, T. A global view of the EDM landscape. Preprint at https://arxiv.org/abs/2403.02052 (2024).
66. Gaul, K. & Berger, R. Global analysis of CP-violation in atoms, molecules and role of medium-heavy systems. *J. High Energy Phys.* **2024**, 100 (2024).
67. Ramsey-Musolf, M. J. & Vasquez, J. C. Left-right symmetry and electric dipole moments. A global analysis. *Phys. Lett. B* **815**, 136136 (2021).
68. Brod, J., Cornell, J. M., Skodras, D. & Stamou, E. Global constraints on Yukawa operators in the standard model effective theory. *J. High Energy Phys.* **2022**, 294 (2022).
69. Aebischer, J., Buras, A. J. & Kumar, J. SMEFT ATLAS: the landscape beyond the Standard Model. Preprint at https://arxiv.org/abs/2507.05926 (2025).
70. Dekens, W. et al. Unraveling models of CP violation through electric dipole moments of light nuclei. *J. High Energy Phys.* **2014**, 69 (2014).
71. Froese, P. & Navrátil, P. Ab initio calculations of electric dipole moments of light nuclei. *Phys. Rev. C* **104**, 025502 (2021).
72. Graner, B., Chen, Y., Lindahl, E. & Heckel, B. Reduced limit on the permanent electric dipole moment of ^{199}Hg. *Phys. Rev. Lett.* **116**, 161601 (2016).
73. Chen, T. et al. Relativistic exact two-component coupled-cluster study of molecular sensitivity factors for nuclear Schiff moments. *J. Phys. Chem. A* **128**, 6540–6554 (2024).
74. Yu, S. S. et al. A conveyor-belt magneto-optical trap of CaF. *Nat. Commun.* **17**, 1175 (2026).
75. Khasanov, S., Su, Y., Safarov, A., Tedila, H. M. & Mamatkulov, O. Major radioactive ion beam facilities: a brief global overview. *Eur. Phys. J. Plus* **140**, 638 (2025).
76. Tarasov, O. B. et al. Observation of new isotopes in the fragmentation of ^{198}Pt at FRIB. *Phys. Rev. Lett.* **132**, 072501 (2024).
77. Abel, E. P. et al. Isotope harvesting at FRIB: additional opportunities for scientific discovery. *J. Phys. G Nucl. Part. Phys.* **46**, 100501 (2019).
78. Patton, B. D. & Robinson, S. M. Minor actinide production at Oak Ridge National Laboratory. In *Proc. Institute of Nuclear Materials Management (INMM) Annual Meeting* https://resources.inmm.org/annual-meeting-proceedings/minor-actinide-production-oak-ridge-national-laboratory (Institute of Nuclear Materials Management, 2019).
79. Collins, E. D. et al. US heavy actinide production at Oak Ridge National Laboratory — ongoing actinide partitioning and transmutation programs. In *Proc. 16th Information Exchange Meeting on Actinide and Fission Product Partitioning and Transmutation (IEMPT 16)* https://www.ornl.gov/publication/us-heavy-actinide-production-oak-ridge-national-laboratory-ongoing-actinide (OECD Nuclear Energy Agency, 2020).
80. Sprouse, G. D. & Orozco, L. A. Laser trapping of radioactive atoms. *Annu. Rev. Nucl. Part. Sci.* **47**, 429–461 (1997).
81. Tandecki, M. et al. Offline trapping of ^{221}Fr in a magneto-optical trap from implantation of an ^{225}Ac ion beam. *J. Instrum.* **9**, P10013 (2014).
82. Fan, M. et al. Laser cooling and trapping of $^{224}Ra^{+}$. *Phys. Rev. Res.* **5**, 043201 (2023).
83. Udrescu, S. M. et al. Isotope shifts of radium monofluoride molecules. *Phys. Rev. Lett.* **127**, 033001 (2021).
84. Wilkins, S. U. et al. Observation of the distribution of nuclear magnetization in a molecule. *Science* **390**, 386 (2025).
85. Udrescu, S. M. et al. Precision spectroscopy and laser-cooling scheme of a radium-containing molecule. *Nat. Phys.* **20**, 202–207 (2024).
86. Athanasakis-Kaklamanakis, M. et al. Electron correlation and relativistic effects in the excited states of radium monofluoride. *Nat. Commun.* **16**, 2139 (2025).
87. Athanasakis-Kaklamanakis, M. et al. Radiative lifetime of the $A^2\Pi_{1/2}$ state in RaF with relevance to laser cooling. *Phys. Rev. A* **110**, L010802 (2024).
88. Athanasakis-Kaklamanakis, M. et al. Laser spectroscopy and CP-violation sensitivity of actinium monofluoride. *Nature* **648**, 562–568 (2025).

89. Hutzler, N. R., Lu, H.-I. & Doyle, J. M. The buffer gas beam: an intense, cold, and slow source for atoms and molecules. *Chem. Rev.* **112**, 4803–4827 (2012).
90. Jadbabaie, A., Pilgram, N. H., Kłos, J., Kotochigova, S. & Hutzler, N. R. Enhanced molecular yield from a cryogenic buffer gas beam source via excited state chemistry. *New J. Phys.* **22**, 022002 (2020).
91. Egorov, D., Lahaye, T., Schöllkopf, W., Friedrich, B. & Doyle, J. M. Buffer-gas cooling of atomic and molecular beams. *Phys. Rev. A* **66**, 043401 (2002).
92. Kaleja, O. et al. The performance of the cryogenic buffer-gas stopping cell of SHIPTRAP. *Nucl. Instrum. Methods Phys. Res.* **463**, 280–285 (2020).
93. Lund, K. et al. Online tests of the advanced cryogenic gas stopper at NSCL. *Nucl. Instrum. Methods Phys. Res. B* **463**, 378–381 (2020).
94. Fitch, N. & Tarbutt, M. Laser-cooled molecules. *Adv. At. Mol. Opt. Phys.* **70**, 157–262 (2021).
95. Augenbraun, B. L. et al. Direct laser cooling of polyatomic molecules. *Adv. At. Mol. Opt. Phys.* **72**, 89–182 (2023).
96. Dilling, J., Blaum, K., Brodeur, M. & Eliseev, S. Penning-trap mass measurements in atomic and nuclear physics. *Annu. Rev. Nucl. Part. Sci.* **68**, 45–74 (2018).
97. Olmschenk, S. et al. Measurement of the lifetime of the $6p\,^2P^o_{1/2}$ level of Yb^+. *Phys. Rev. A* **80**, 022502 (2009).
98. Rosch, D., Wenz, H., Kalkstein, M., Kracke, A. & Vogel, M. Design and characterization of a linear quadrupole ion trap for the investigation of cold molecular ions. *EPJ Tech. Instrum.* **3**, 5 (2016).
99. Hermanspahn, N. et al. Observation of the continuous Stern–Gerlach effect on an electron bound in an ion. *Phys. Rev. Lett.* **84**, 427–430 (2000).
100. Rosenband, T. et al. Frequency ratio of Al^+ and Hg^+ single-ion optical clocks; metrology at the 17th decimal place. *Science* **319**, 1808 (2008).
101. Schmidt, P. O. et al. Spectroscopy using quantum logic. *Science* **309**, 749 (2005).
102. Wolf, F. et al. Non-destructive state detection for quantum logic spectroscopy of molecular ions. *Nature* **530**, 457–460 (2016).
103. Chou, C.-W. et al. Preparation and coherent manipulation of pure quantum states of a single molecular ion. *Nature* **545**, 203–207 (2017).
104. Chou, C.-W. et al. Frequency-comb spectroscopy on pure quantum states of a single molecular ion. *Science* **367**, 1458–1461 (2020).
105. Calvin, A. et al. Single molecule infrared spectroscopy in the gas phase. *Nature* **621**, 295–299 (2023).
106. Moses, S. A. et al. A race-track trapped-ion quantum processor. *Phys. Rev. X* **13**, 041052 (2023).
107. Xu, S. et al. 3D-printed micro ion trap technology for quantum information applications. *Nature* **645**, 362–368 (2025).
108. Chen, J.-S. et al. Sympathetic ground state cooling and time-dilation shifts in an $Al27^+$ optical clock. *Phys. Rev. Lett.* **118**, 053002 (2017).
109. Pagano, G. et al. Cryogenic trapped-ion system for large scale quantum simulation. *Quantum Sci. Technol.* **4**, 014004 (2019).
110. Verma, M., Jayich, A. M. & Vutha, A. C. Electron electric dipole moment searches using clock transitions in ultracold molecules. *Phys. Rev. Lett.* **125**, 153201 (2020).
111. Zhang, C., Yu, P., Jadbabaie, A. & Hutzler, N. R. Quantum-enhanced metrology for molecular symmetry violation using decoherence-free subspaces. *Phys. Rev. Lett.* **131**, 193602 (2023).
112. Kozyryev, I. & Hutzler, N. R. Precision measurement of time-reversal symmetry violation with laser-cooled polyatomic molecules. *Phys. Rev. Lett.* **119**, 133002 (2017).
113. Yu, P. & Hutzler, N. R. Probing fundamental symmetries of deformed nuclei in symmetric top molecules. *Phys. Rev. Lett.* **126**, 023003 (2021).
114. Fan, M. et al. Optical mass spectrometry of cold $RaOH^+$ and $RaOCH_3^+$ $RaOCH_3^{\ddagger}$. *Phys. Rev. Lett.* **126**, 023002 (2021).
115. Zülch, C., Gaul, K., Giesen, S. M., Garcia Ruiz, R. F. & Berger, R. Cool molecular highly charged ions for precision tests of fundamental physics. Preprint at https://arxiv.org/abs/2203.10333 (2022).
116. Fan, X., Myers, T. G., Sukra, B. A. D. & Gabrielse, G. Measurement of the electron magnetic moment. *Phys. Rev. Lett.* **130**, 071801 (2023).
117. Karthein, J. et al. Electroweak nuclear properties from single molecular ions in a penning trap. *Phys. Rev. Lett.* **133**, 033003 (2024).
118. Shuman, E. S., Barry, J. F. & DeMille, D. Laser cooling of a diatomic molecule. *Nature* **467**, 820–823 (2010).
119. Isaev, T., Hoekstra, S. & Berger, R. Laser-cooled RaF as a promising candidate to measure molecular parity violation. *Phys. Rev. A* **82**, 052521 (2010).
120. Isaev, T. A., Zaitsevskii, A. V. & Eliav, E. Laser-coolable polyatomic molecules with heavy nuclei. *J. Phys. B* **50**, 225101 (2017).
121. Zhang, C., Yu, P., Conn, C. J., Hutzler, N. R. & Cheng, L. Relativistic coupled-cluster calculations of RaOH pertinent to spectroscopic detection and laser cooling. *Phys. Chem. Chem. Phys.* **25**, 32613–32621 (2023).
122. Lasner, Z. D. et al. Magneto-optical trapping of a heavy polyatomic molecule for precision measurement. *Phys. Rev. Lett.* **134**, 083401 (2025).
123. Bohn, J. L., Rey, A. M. & Ye, J. Cold molecules: progress in quantum engineering of chemistry and quantum matter. *Science* **357**, 1002–1010 (2017).
124. Meyer, E. R. & Bohn, J. L. Electron electric-dipole-moment searches based on alkali-metal-or alkaline-earth-metal-bearing molecules. *Phys. Rev. A* **80**, 042508 (2009).
125. Fleig, T. & DeMille, D. Theoretical aspects of radium-containing molecules amenable to assembly from laser-cooled atoms for new physics searches. *New J. Phys.* **23**, 113039 (2021).
126. Kłos, J., Li, H., Tiesinga, E. & Kotochigova, S. Prospects for assembling ultracold radioactive molecules from laser-cooled atoms. *New J. Phys.* **24**, 025005 (2022).
127. Marc, A., Hubert, M. & Fleig, T. Candidate molecules for next-generation searches of hadronic charge–parity violation. *Phys. Rev. A* **108**, 062815 (2023).
128. Marc, A. & Fleig, T. Semi-hadronic charge–parity violation interaction constants in CsAg, FrLi and FrAg molecules. *Eur. Phys. J. D* **79**, 19 (2025).
129. Vayninger, M. et al. Magneto-optical trap of silver and potassium atoms. *Phys. Rev. A* **112**, 063306 (2025).
130. Liu, L. et al. Building one molecule from a reservoir of two atoms. *Science* **360**, 900–903 (2018).
131. Cairncross, W. B. et al. Assembly of a rovibrational ground state molecule in an optical tweezer. *Phys. Rev. Lett.* **126**, 123402 (2021).
132. Vutha, A. C., Horbatsch, M. & Hessels, E. A. Orientation-dependent hyperfine structure of polar molecules in a rare-gas matrix: a scheme for measuring the electron electric dipole moment. *Phys. Rev. A* **98**, 032513 (2018).
133. Singh, J. T. A new concept for searching for time-reversal symmetry violation using Pa-229 ions trapped in optical crystals. *Hyperfine Interact.* **240**, 392 (2019).
134. Ramachandran, H. D. & Vutha, A. C. Nuclear *T*-violation search using octopole-deformed nuclei in a crystal. *Phys. Rev. A* **108**, 012819 (2023).
135. Morris, I. M. et al. Rare isotope-containing diamond colour centres for fundamental symmetry tests. *Philos. Trans. R. Soc. A* **382**, 20230169 (2023).
136. Van Vleck, J. H. The dipolar broadening of magnetic resonance lines in crystals. *Phys. Rev.* **74**, 1168–1183 (1948).
137. Kittel, C. & Abrahams, E. Dipolar broadening of magnetic resonance lines in magnetically diluted crystals. *Phys. Rev.* **90**, 238–239 (1953).
138. Royce, E. B. & Bloembergen, N. Linear electric shifts in the paramagnetic resonance of Al_2O_3:Cr and MgO:Cr. *Phys. Rev.* **131**, 1912–1923 (1963).
139. Mims, W. B. *The Linear Electric Field Effect in Paramagnetic Resonance* (Clarendon Press, 1976).
140. Yang, X., Wang, S., Wilkins, S. & Ruiz, R. G. Laser spectroscopy for the study of exotic nuclei. *Prog. Part. Nucl. Phys.* **129**, 104005 (2023).
141. Kamiński, T. et al. Astronomical detection of radioactive molecule ^{26}AlF in the remnant of an ancient explosion. *Nat. Astron.* **2**, 778–783 (2018).
142. Moller, P., Sierk, A. J., Ichikawa, T. & Sagawa, H. Nuclear ground-state masses and deformations: FRDM(2012). *At. Data Nucl. Data Tables* **109–110**, 1–204 (2016).
143. Kwon, H. Supersymmetry searches at ATLAS and CMS. Preprint at https://arxiv.org/abs/2506.06839 (2025).
144. The ATLAS Collaboration. The quest to discover supersymmetry at the ATLAS experiment. *Phys. Rep.* **1116**, 261–300 (2024).
145. Sekmen, S. Supersymmetry searches in CMS run 2: a complete review. *High. High Energy Phys.* **1**, 18 (2025).
146. Jayich, A. EDM-limits. *Zenodo* https://doi.org/10.5281/zenodo.20278872 (2025).

Acknowledgements
A.J. acknowledges support from the National Science Foundation (PHY-2402254). R.F.G.R. acknowledges support from the US Department of Energy, Office of Science, Office of Nuclear Physics under grants DE-SC0021176 and DE-SC0021179 and the Center for Ultracold Atoms (an NSF Physics Frontier Center). N.R.H. acknowledges support from the National Science Foundation (PHY-2309361 and CAREER PHY-1847550) and the Heising–Simons Foundation (2022-3361). A.M.J. acknowledges support from the Department of Energy DE-SC0022034, the National Science Foundation PHY-2146555 and the Heising–Simons Foundation 2022-4066. J.T.S. acknowledges support from the US Department of Energy, Office of Science, Office of Nuclear Physics, under contracts DE-SC0019015, DE-SC0019455 and DE-SC0025679. The authors thank D. DeMille for discussions and his input for Fig. 3.

Author contributions
All authors contributed to all aspects of this work.

Competing interests
The authors declare no competing interests.

Additional information

Supplementary information The online version contains supplementary material available at https://doi.org/10.1038/s42254-026-00950-9.

Peer review information *Nature Reviews Physics* thanks the anonymous reviewers for their contribution to the peer review of this work.